Iranian Journal of Geophysics, Vol 19, No 6, 2025, P. 1 (Research article)
DOI: 10.30499/ijg.2025.502304.1675

Uncertainty estimation in Earthquake Magnitude Determination Using High-Rate GPS Data with Bootstrap method

Sara Bahrami Asl[1], Khalil Bakhtiari Asl[1], Khosro Moghtased- Azar[1]

[1]Department of Geomatics Engineering, Faculty of Civil Engineering, University of Tabriz, Tabriz, Iran

Abstract

Accurate analysis of earthquake magnitude and evaluation of its associated uncertainty are fundamental topics in seismology and disaster management. In this study, the earthquake magnitudes were estimated using high-rate GPS data for three major events: the 2011 Tohoku earthquake (Mw 9.1), the 2021 Chignik earthquake (Mw 8.2), and the 2018 Anchorage earthquake (Mw 7.1). The final estimated magnitudes using the proposed method were approximately Mw 9.25 for Tohoku, Mw 8.27 for Chignik, and Mw 7.08 for Anchorage, closely aligning with official reports. High-rate GPS data, due to their ability to precisely capture real-time crustal displacements, were utilized as the primary data source. These data provided valuable information on maximum displacement, dominant period, and epicentral distance, and were employed for estimating earthquake magnitude and analyzing uncertainty. To analyze the data, combinations of different GPS stations were used to minimize the impact of noisy data and achieve more stable results. The application of the Bootstrap statistical method reduced uncertainty values significantly from approximately 0.0039 to 0.0011 for Tohoku, 0.0031 to 0.0019 for Chignik, and 0.004 to 0.0015 for Anchorage. These results demonstrate the statistical robustness and effectiveness of the proposed approach. Compared to conventional seismic methods, which suffer from data clipping and saturation for large magnitudes, the high-rate GPS method provided stable and unbiased magnitude estimates without signal saturation issues. The findings underscore the importance of expanding GPS networks in tectonically active regions, integrating seismic and GPS data, and employing advanced algorithms for data processing. Furthermore, the research emphasizes the role of comprehensive data analysis in improving early earthquake warning systems. By incorporating high-rate GPS data with traditional seismic data, the precision and reliability of early warning systems can be significantly enhanced, ultimately reducing the potential for loss of life and property. Additionally, this study highlights the necessity of strengthening infrastructure resilience and investing in advanced monitoring technologies. In conclusion, this research successfully demonstrates that high-rate GPS data, combined with the Bootstrap method, can accurately estimate earthquake magnitudes, reduce uncertainty, and enhance the reliability of seismic assessments. These findings contribute to the development of more effective earthquake early warning systems and risk mitigation strategies.

Key words: High- rate GPS, Bootstrap, Earthquake Magnitude

Introduction

Seismology is one of the branches of geophysics that deals with the scientific study of earthquakes and the propagation of elastic waves in the earth and other planetary bodies. This science plays a vital role in understanding the behavior and characteristics of seismic events, which is necessary to assess the risks caused by it and design structures that can withstand possible earthquakes.

One of the main goals of seismology is to accurately determine the source characteristics of earthquakes, including their magnitude, location and focal mechanism (Bakhtiari Asl, et al. 2025) and (Salmanian et al. 2025). To achieve this goal, seismologists use various techniques and methods, among which high-rate GPS data plays an essential role.

The reliable and fast measurement of the magnitude of an earthquake is a challenging problem, especially for large earthquakes (≥8). Currently, the magnitude of an earthquake is measured using devices such as seismographs and accelerometers, but these devices have limitations in correctly measuring the magnitude of earthquakes that are greater than Mw8. However, it is important to clarify that the saturation or clipping issue primarily affects certain magnitude scales such as body-wave magnitude (Mb) and surface-wave magnitude (Ms), which rely on limited frequency bands and waveform characteristics. In contrast, the moment magnitude scale (Mw), which is based on seismic moment and total energy release, is specifically designed to avoid saturation and remains reliable even for very large earthquakes. In the measurement of large earthquakes using Mb and Ms Scales, seismograph devices face the problem of saturation or clipping in the measured data (Kulhánek 2002). In such cases, it is not possible to record the full range of speed or acceleration.

The displacements caused by earthquakes can be measured directly with GPS, while in seismometers for calculating the displacement, the velocity data must be integrated once and the acceleration data twice. This process increases error and amplifies the noise, which ultimately distorts the real signal (Boore et al. 2002). Besides that, seismometers face the problem of clipping in the measurement data when strong ground movements occur. When the signal is clipped, it is not possible to accurately and correctly record the maximum amplitude of the ground vibration. But unlike seismometers, GPS observations do not clip due to the absence of any limitations in the device's response (Bilich 2006).

Until now, many people have utilized high-rate GPS data for earthquake source parameter studies. For instance (Hirahara et al. 1995) used dual-frequency GPS devices and kinematic techniques to study earthquake-induced displacements. Despite 11 cm orbital errors, they recorded horizontal displacements with 1-2 cm accuracy at a 161 km distance from the earthquake source.

(Elósegui et al. 2006) evaluated high-rate GPS accuracy for seismology. Using earthquake simulation, they controlled GPS antenna movement to reconstruct ground displacements. Results showed a GPS error of about 1.5mm, with 16% of data having less than 5mm error. The errors appeared as noise lasting approximately 6.2 seconds. Increasing the GPS sampling rate beyond a certain limit did not provide additional useful information for distant earthquakes. These findings indicate that optimized GPS technology can accurately analyze ground movements during earthquakes.

(Bilich et al. 2008) analyzed high-rate GPS data for earthquake displacement. Using 1 Hertz sampling GPS data, geodetic models,

and GIPSY software, they found GPS could measure dynamic surface displacements and movements larger than several tens of centimeters near faults, recording up to 1 meter in the Denali Fault earthquake. GPS data did not saturate large earthquakes, accurately measuring displacement changes.

(Colombelli, Allen et al. 2013) studied GPS data for early earthquake warning. Using an algorithm to extract permanent ground displacements from GPS time series and refine rupture models based on preliminary estimates, they found that GPS provided accurate magnitude estimates and better ground shaking predictions. For the 1122 Tohoku-Oki earthquake, the initial magnitude estimates of 8.1 was refined to 8.8 within 211 seconds. This method also significantly improved the accuracy and speed of tsunami warnings.

(Gao, Li et al. 2021) assessed the magnitude estimation of the Maduo earthquake using high-rate GNSS data. Utilizing 55 GNSS stations and applying relative positioning and variometric methods, they found the magnitude estimates from maximum ground displacement to be Mw 7.25 and maximum ground velocity to be approximately Mw 7.31, aligning with the USGS-reported Magnitude with error of 0.05 and 0.01 magnitude units.

(Lamarre et al. 1992) studied the use of the bootstrap method to quantify uncertainty in seismic hazard estimates. They combined uncertainties from earthquake catalogs, magnitude scales, and models to provide confidence intervals and a comprehensive analysis. Results showed the bootstrap method effectively assessed uncertainty and improved estimate accuracy, leading to a thorough analysis of seismic hazards. This paper aims to quantify the uncertainty of high-rate GPS data in rapid estimation of earthquake magnitudes using the bootstrap method.

Data and Case Studies

For applying the methods, high- rate GPS data from SOPAC- Garner[1] was used to calculate uncertainty in earthquake magnitude estimation for three study areas: Tohoku 2011, Chignik 2021 and Anchorage 2018 earthquake.

1) Tohoku 2011 Earthquake

On March 11, 2011, at 14:46 local time (10:46 UTC), a 9.1 magnitude earthquake struck off the eastern coast of Japan, in the Tohoku region with the latitude and longitude of 38.29°N and 142.37°E. The earthquake, also known as the Great East Japan Earthquake, was one of the strongest ever recorded in Japan's history. It triggered a devastating tsunami that caused widespread damage to coastal areas.

The Tohoku earthquake was the result of the subduction of the Pacific Plate beneath the Eurasian Plate in a subduction zone. This subduction occurred at the western edge of the Japan Trench. The earthquake's focal mechanism was characterized as a thrust fault, where the oceanic plate moved downward along an inclined fault surface (Chen et al. 2014).

In Figure 1, the location of the earthquake's epicenter, the faults in the region, and the locations of the stations used for calculating the magnitude of the Tohoku earthquake are shown. A total of 40 GPS stations were used for this earthquake.

[1] Scripps Orbit and Permanent Array Center (garner.ucsd.edu)

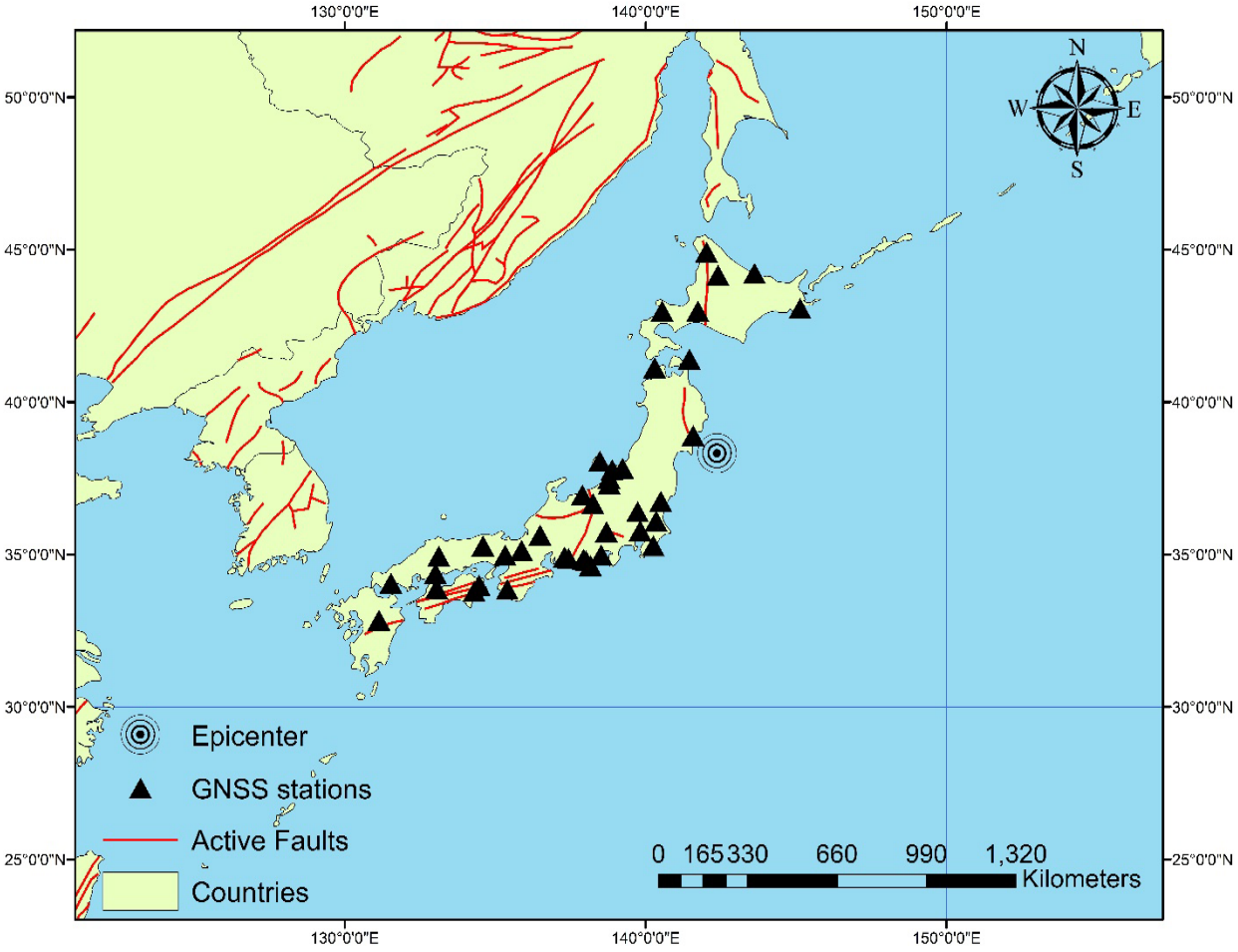

Figure 1- The location of the earthquake's epicenter, the faults in the region, and the locations of the stations used for calculating the magnitude of the Tohoku earthquake

2) Chignik 2021 Earthquake

On July 18, 2021, at 11:10 PM local time (16:10 UTC on July 19), an 8.2 magnitude earthquake occurred off the coast of Chignik, Alaska, at a depth of 31 km with the latitude of 55.36°N and longitude of -158.88°W. Despite its high magnitude, the remote location and low population density meant there were no significant casualties or damage. The earthquake triggered a tsunami warning, later canceled. This event was the largest recorded in the United States in over 50 years, emphasizing the need for monitoring and preparedness. The Chignik earthquake was a megathrust event in a subduction zone where the Pacific Plate subducts beneath the North American Plate. It caused significant displacements in the ocean bed and Earth's crust (Konvisar et al. 2024). In Figure 2, the location of the earthquake's epicenter, the faults in the region, and the locations of the stations used to calculate the magnitude of the Chignik earthquake are shown. For this earthquake, 48 stations were used for calculations.

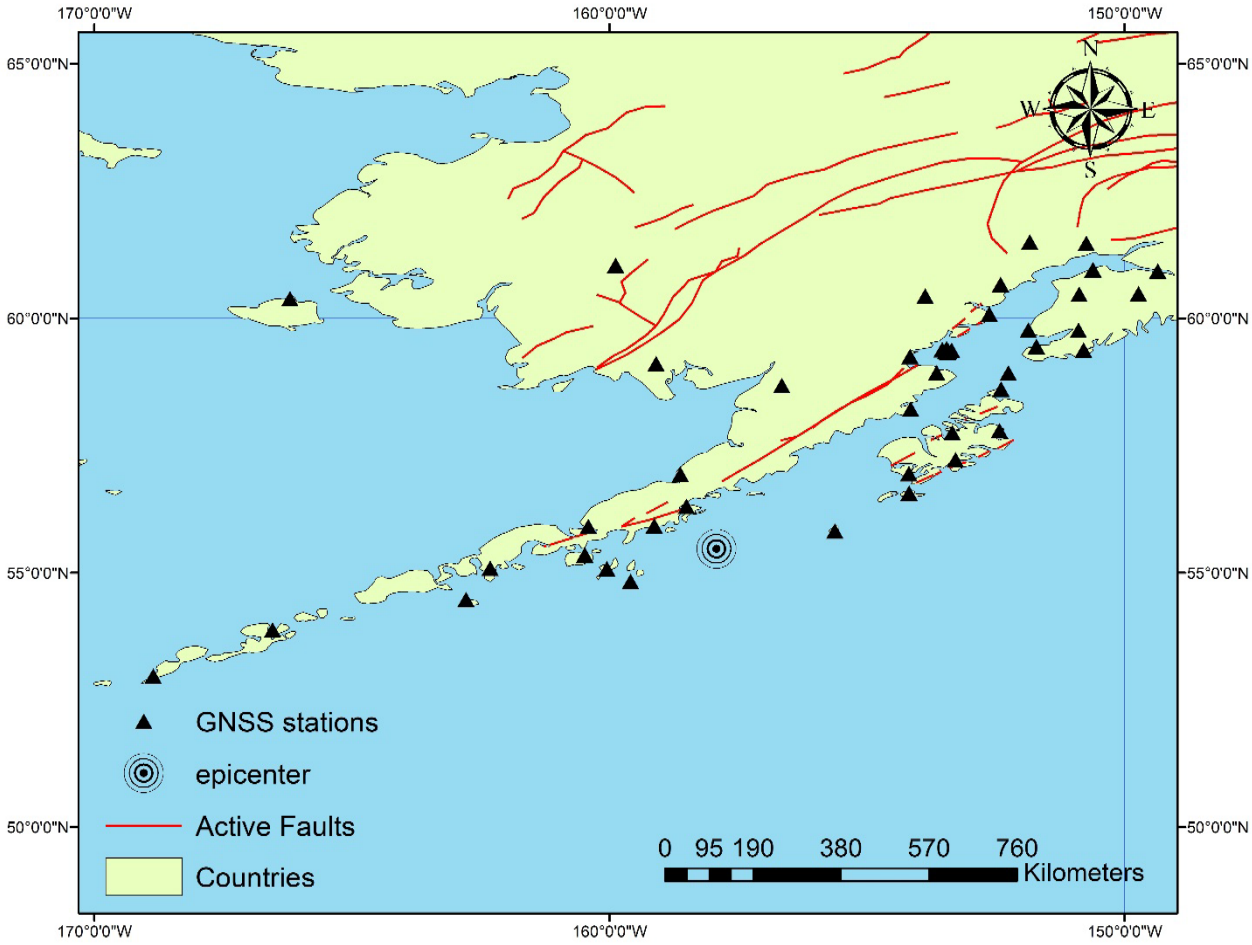

Figure 2- The location of the earthquake's epicenter, the faults in the region, and the locations of the stations used for calculating the magnitude of the Chignik earthquake

3) Anchorage 2018 Earthquake

On November 30, 2018, at 8:19 AM local time (17:29 UTC), a 7.1 magnitude earthquake occurred near Anchorage, Alaska, at a latitude of 61.36°N and a longitude of 149.95°W. The epicenter of this earthquake was at a depth of 47 km, approximately 16 km north of Anchorage. The earthquake was caused by accumulated stresses at the boundary between the Pacific and North American plates. The focal mechanism indicated a thrust fault with a compressive component, a type of fault commonly observed in subduction zones like Alaska, where the Pacific Oceanic Plate subducts beneath the North American Plate. The maximum ground displacement was recorded near the earthquake's epicenter (West et al. 2020). In Figure 3, the location of the earthquake's epicenter, the faults in the region, and the locations of the stations used to calculate the magnitude of the Anchorage earthquake are shown. For this earthquake, 48 stations were used for calculations

.

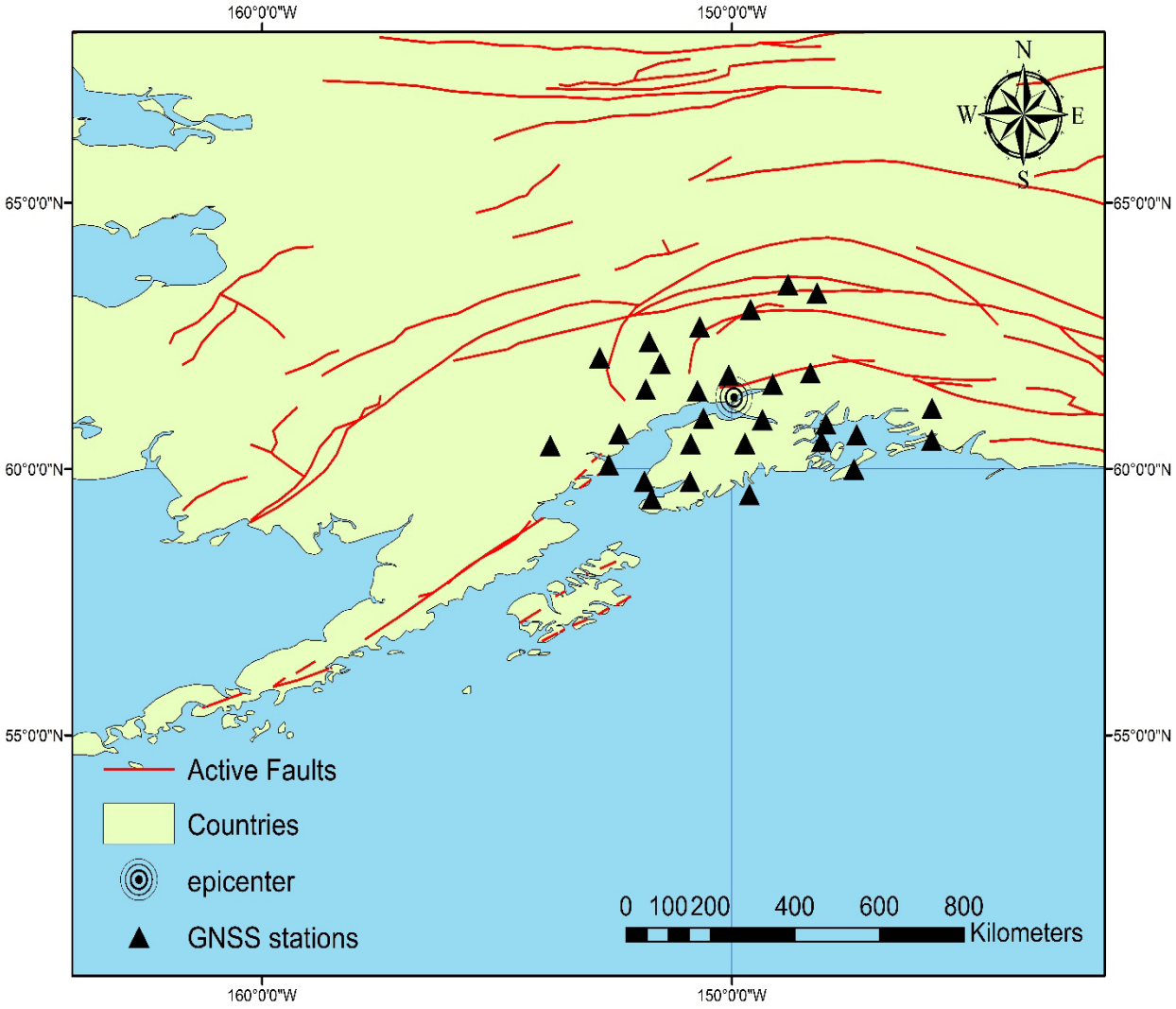

Figure 3- The location of the earthquake's epicenter, the faults in the region, and the locations of the stations used for calculating the magnitude of the Chignik earthquake

The data we used here include displacement information recorded by GPS stations, essential for earthquake analysis. Files in the designated path are read separately, and each station's information is stored in an organized structure. Station names are also extracted and categorized for use in processing and analysis. This foundational step prepares the data for subsequent calculations, such as earthquake magnitude estimation and uncertainty analysis.

.

Precise data organization ensures efficient access and usability for calculations and analyses. For example, Figure 4 shows the data recorded by the SLED station for the Chignik earthquake on July 18, 2021, which includes the displacement of the Earth's crust in three main components. Recorded data for all GPS stations in all three study areas was available and extracted for all three components

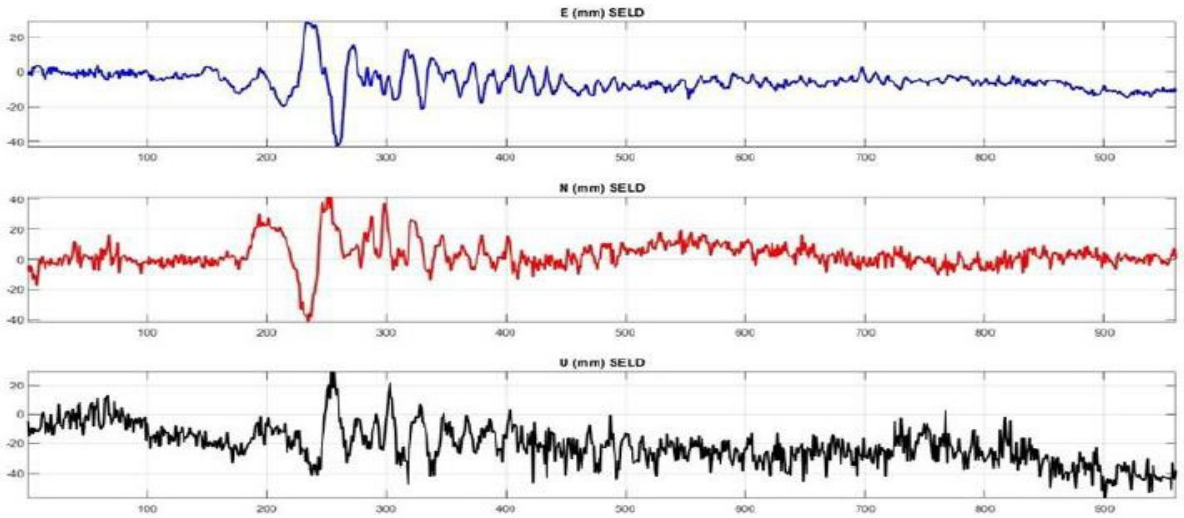

Figure 4- Time series of horizontal and vertical components for the SLED station. The x axis represents the time and the y axis shows displacement in millimeters. (Latitude: 61.59°N and longitude 149.13°W)

Although the Bootstrap method is a well-established statistical technique, its application to high-rate GPS data for earthquake magnitude estimation is still limited. This study explores its effectiveness for uncertainty quantification and convergence behavior using three large earthquakes, providing insights that are directly applicable to near-real-time geodetic monitoring and early warning systems.

Methodology

One of the common and well-known methods for determining earthquake magnitude is the Gutenberg relationship, which estimates earthquake magnitude based on seismic data (Fang et al. 2014). This method uses the maximum wave amplitude recorded on seismographs and its distance from the earthquake's epicenter to calculate the magnitude. However, this method has limitations, including issues with amplitude saturation in large earthquakes (greater than 8) and the inability to fully record crustal displacements, especially in earthquakes near active faults.

$$\mathrm{M} = \log(\mathrm{A}) + 1.66\log(\Delta) + 2.0 \qquad (1)$$

In the above relation, A is the maximum displacement recorded by the device at a specific station. This displacement can be in either the vertical or horizontal direction and is measured via GPS or a seismograph. Δ is the epicentral distance between the data recording station and the earthquake's epicenter. This distance is usually expressed in kilometers and calculated from geographical coordinates using geometric formulas such as the Haversine formula. The coefficient 1.66 reflects the impact of epicentral distance on earthquake magnitude, and the coefficient +2 is a constant to adjust the scale and align it with the standard earthquake magnitude scale.

$$\Delta = 2r\,.\arcsin\left(\sqrt{sin^2\left(\frac{\phi_2-\phi_1}{2}\right)+cos(\phi_1)\,cos(\phi_2)\,sin^2\left(\frac{\lambda_2-\lambda_1}{2}\right)}\right)$$

In the above relation, which is used to calculate the epicentral distance between the data recording station and the earthquake's epicenter, **r** represents the radius of the Earth, and **ϕ** and **λ** are the latitude and longitude, respectively.

$$C(n,k) = \binom{n}{k} = \frac{n!}{k!\,(n-k)!} \qquad (3)$$

Combinatorics k from n refers to the number of ways to choose **k** elements from a set of **n** elements without considering the order. In the above relation, the order of the selected elements does not matter. Combinations are one of the fundamental tools in statistics and data analysis for sampling and simulation (Roberts and Tesman 2024). In this study, GPS data from **n** stations were collected, each providing information about crustal displacements. However, using data from all stations may not always be practical or optimal. The reasons for using combinations of **k** from **n** in this study include:

1) Optimization of analyses: Given time or processing constraints, it is necessary to select a subset of the n stations rather than using all of them. Combinations of k from n allow for the creation of all possible combinations of k stations for analysis, thereby enabling the examination of the impact of different station combinations on the result (such as earthquake magnitude).

2) Reducing sensitivity to noisy or faulty data: Some stations may have recorded data with high noise levels or low accuracy. By selecting different combinations of stations, the impact of unreliable data is reduced, resulting in more reliable outcomes.

3) Assessing result stability: Analyzing different combinations of stations allows for evaluating the stability of results and the impact of adding or removing stations on earthquake magnitude calculations. This is done by averaging the results of the different combinations.

For studying the uncertainty, the Bootstrap method was used. The concept of uncertainty arises due to the presence of noise, instrument errors, and inherent data limitations. In statistics, uncertainty is one of the key concepts that help evaluate the accuracy and reliability of results. To understand and express uncertainty, statistical measures such as the mean, standard deviation, and confidence interval are used, which provide valuable information about data distribution and variability. In uncertainty analysis, the mean (equation 4) is used as a baseline to evaluate data deviation from the center. For example, in earthquake analysis, the average magnitude calculated from various station combinations can represent the actual earthquake magnitude. Data with similar means indicate stability and consistency of results, while large mean differences suggest the presence of errors or noise.

$$\bar{M} = \frac{1}{N}\sum_{i=1}^{N} M_i \qquad (4)$$

Standard deviation is a measure of the dispersion of data around the mean. This metric indicates how much the data deviates from the mean value:

$$\sigma_M = \sqrt{\frac{\sum_{i=1}^{N}(M_i - \bar{M})^2}{N}} \qquad (5)$$

Data with low standard deviation indicates low dispersion and high accuracy of the results, while high standard deviation suggests possible fluctuations or errors. In uncertainty analysis, standard deviation is used as an indicator to evaluate the overall accuracy of calculations. For example, in earthquake magnitude analysis, low standard deviation in different station combinations indicates the reliability of the results.

In earthquake studies, uncertainty in calculating earthquake magnitude is of great importance. If GPS or seismographic data have noise or dispersion, this can lead to unstable calculations. Uncertainty analysis in this case involves examining the impact of data noise, changes in the mean, and standard deviation on the results.

Bootstrap is a statistical method based on resampling, used to estimate uncertainty and the statistical distribution of values. This method is particularly useful when access to many samples is not possible or specific distributional assumptions are not met (Lamarre, Townshend et al. 1992).

In this study, the Bootstrap method was used to examine uncertainty in calculating earthquake magnitude using GPS data. The steps are as follows:

1) Input data: Displacement data from GPS stations were used as input for calculating earthquake magnitude. This data may be noisy or affected by systematic errors.

2) Creating resampled samples: Resampled samples for calculating the average earthquake magnitude were created from various station combinations. This process was done randomly and with replacement.

Overall, if we want to summarize the methodology, in this study, a comprehensive approach was employed to accurately determine earthquake magnitude and analyze related uncertainties. This approach combines high-sampling-rate GPS data, the empirical Gutenberg relationship, station combinations, and the statistical Bootstrap method.

First, displacement data from GPS stations, which record real-time crustal movements, were collected. These data include information on maximum displacement (A), dominant frequency (T), and epicentral distance (Δ), each of which is applied to the generalized empirical Gutenberg relationship. This relationship allows for high-accuracy earthquake magnitude estimation without the limitations caused by seismograph saturation or noise.

To reduce the impact of noisy data and assess result stability, combinations of kk from nn GPS stations were analyzed. This process involves selecting various subsets of GPS stations and calculating earthquake magnitude for each possible combination. For example, if there are nn GPS stations, all possible combinations of kk stations are selected, and the earthquake magnitude is calculated for each combination. This method allows for the analysis of the impact of different station combinations on results and the assessment of result stability in the presence of uncertain data.

Finally, the Bootstrap method was used to evaluate uncertainty. This statistical method generates resampled samples of earthquake magnitude values obtained from different combinations. In each step of this process, a random set of data is selected, and the average earthquake magnitude is calculated. By repeating this process for many samples (typically 1000 or more), a statistical distribution of the calculated averages is obtained. The standard deviation of this distribution is reported as the measure of earthquake magnitude uncertainty.

However, it is important to recognize that completely random selection of stations may not always produce representative results. During an earthquake, the energy and displacement fields propagate outward from the epicenter, resulting in significant differences between near-field and far-field stations. Near-field stations typically experience higher displacements earlier, while far-field stations may record delayed and attenuated signals. Furthermore, the fault's rupture orientation and source radiation pattern cause directional variations in recorded ground motions, leading some stations to experience larger displacements than others depending on their azimuthal positions relative to the rupture.

To improve the robustness of the Bootstrap analysis, future studies should consider stratified sampling strategies that account for these physical phenomena. This includes ensuring balanced inclusion of both near-field and far-field stations and factoring in the azimuthal distribution relative to the fault mechanism. Incorporating these considerations will lead to a more representative dataset and enhance the accuracy and reliability of magnitude estimation.

This combined approach not only enhances the accuracy of earthquake magnitude estimation but also provides precise information about the stability and reliability of the results. Overall, this method, which integrates precise GPS data, combinatorial analysis, and advanced statistical

methods like Bootstrap, offers a powerful tool for analyzing large earthquakes, seismic modeling, and earthquake risk assessment. The results of this study can be highly effective in earthquake early warning systems and crisis management planning. In figure 8 shows a complete flowchart of proposed method.

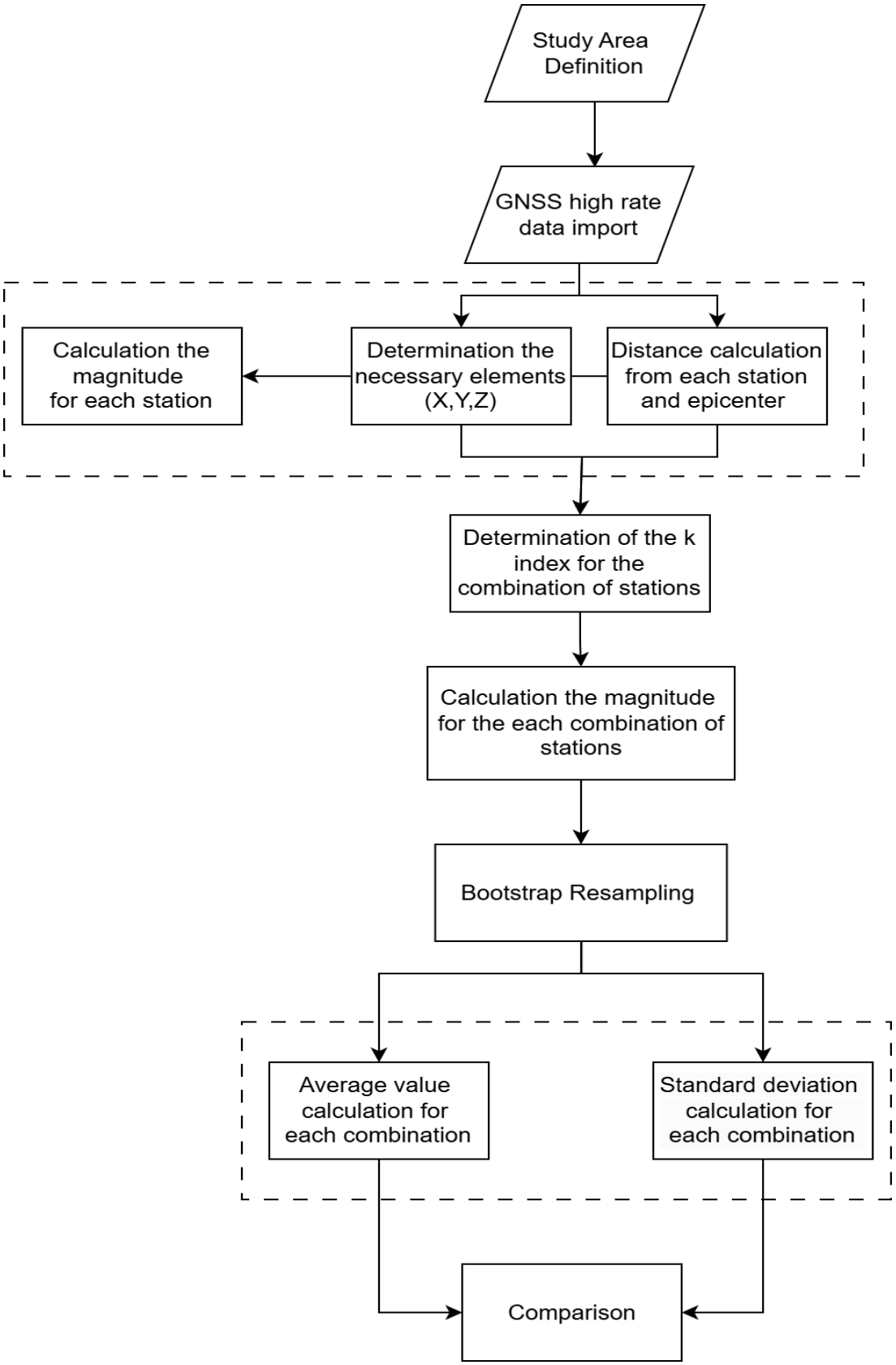
Study Area Definition
GNSS high rate data import
Calculation the magnitude for each station
Determination the necessary elements (X,Y,Z)
Distance calculation from each station and epicenter
Determination of the k index for the combination of stations
Calculation the magnitude for the each combination of stations
Bootstrap Resampling
Average value calculation for each combination
Standard deviation calculation for each combination
Comparison

Figure 5- Flowchart of proposed method

Implementations and Results

Figure 6 shows the analysis of high-rate GPS data for the 2011 Tohoku earthquake. This figure includes three parts that present the process of earthquake magnitude calculation, the average results for different station combinations, and the associated uncertainty assessment.

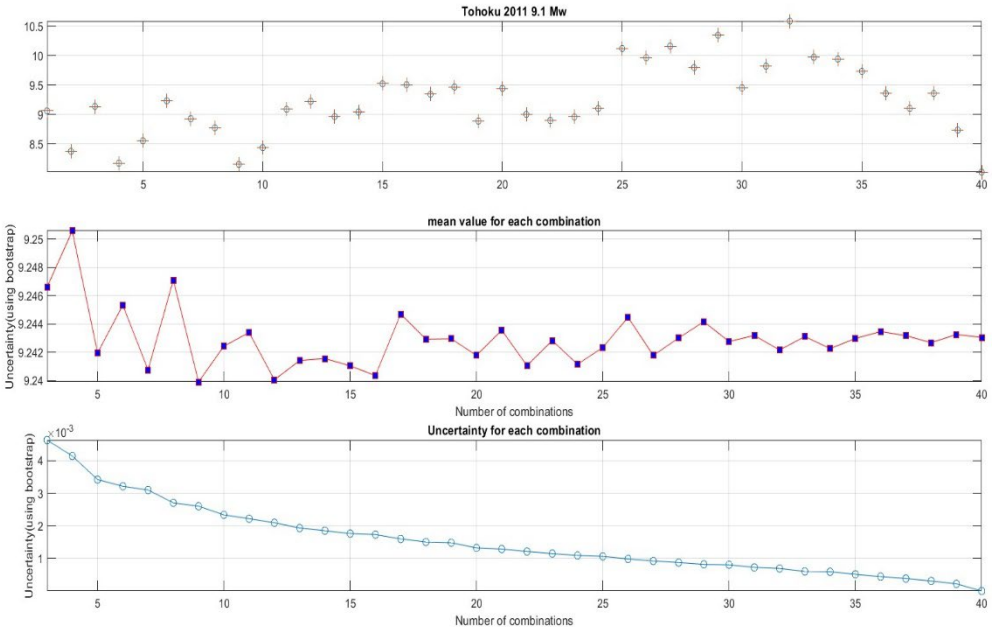

Figure 6- Magnitude estimation results for theTohoku earthquake. The top panel shows the variation in magnitude values (y-axis) for different numbers of randomly selected stations (x-axis). The middle panel presents the distribution of magnitude estimates (y-axis) across multiple Bootstrap resampling combinations for each station count (x-axis). The bottom panel shows the standard deviation of the magnitude estimates (uncertainty, y-axis)) computed from the Bootstrap samples (x-axis).

Part 1: Magnitude of Earthquake for Selected Stations In the first chart, the calculated earthquake magnitude (M) for each GPS station is shown. Each point represents the calculated magnitude for the data of a station. The magnitude values vary between approximately 8.25 and 10.5. These variations are due to differences in data recorded by the stations and their geographical locations relative to the earthquake's epicenter.

Part 2: Average Magnitude for Each Selected Combination of Stations The second chart shows the average earthquake magnitude for different numbers of stations in the calculated combinations. The horizontal axis displays the number of selected stations in each combination, while the vertical axis shows the average calculated magnitude for that number of combinations. The chart's behavior indicates that as the number of stations in each combination increases, the calculated average magnitude converges towards a more stable and consistent value (approximately 9.25) and The tendency towards stability and consistency in the average is due to the reduction in the impact of noisy or unreliable data in the averaging process.

Part 3: Calculating Uncertainty for Each Combination (Bootstrap) The third chart shows

the standard deviation of the calculated results for each combination, which is considered uncertainty. As the number of selected stations in the combinations increases the uncertainty decreases, because combining a larger number of stations leads to more stable results. Also, in combinations with fewer stations, the uncertainty is higher (in the range of 0.0039), but it decreases to about 0.001 as the number of stations increases.

Figure 7, like the previous figure shows the analysis of high- rate GPS data on Chignik 2021 earthquake.

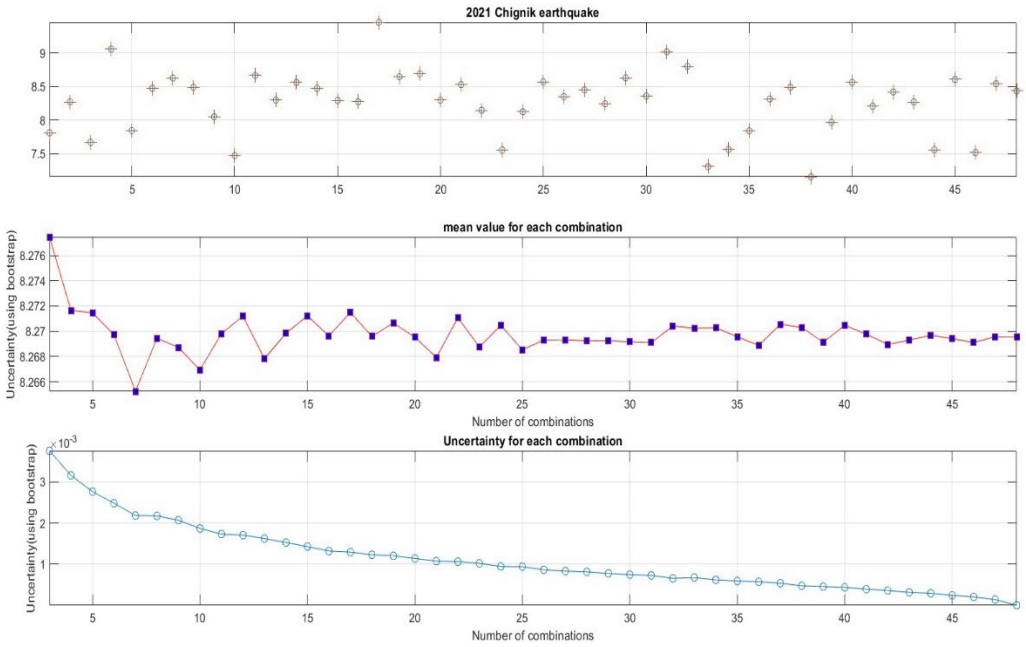

Figure 7- Magnitude estimation results for the Chignik earthquake. The top panel shows the variation in magnitude values (y-axis) for different numbers of randomly selected stations (x-axis). The middle panel presents the distribution of magnitude estimates (y-axis) across multiple Bootstrap resampling combinations for each station count (x-axis). The bottom panel shows the standard deviation of the magnitude estimates (uncertainty, y-axis)) computed from the Bootstrap samples (x-axis).

In the first chart of figure 10, the calculated earthquake magnitude (M) for each GPS station is shown. Each point represents the calculated magnitude for the data of a station. The magnitude values vary between approximately 7.5 and 9.0. These variations are due to differences in data recorded by the stations and their geographical locations relative to the earthquake's epicenter.

In the second chart, the average earthquake magnitude for various station combinations is calculated and displayed. The horizontal axis shows the number of combinations, and the vertical axis shows the average magnitude values for those combinations. It is observed that the average earthquake magnitude approaches a constant value (approximately 8.27) as the number of station combinations increases. This trend indicates the stability of the results and the reduction in the impact of noisy or unreliable data in larger combinations.

The third chart shows the standard deviation of the earthquake magnitude values for different station combinations, calculated using the Bootstrap method. The horizontal axis shows the number of combinations, and the vertical axis shows the calculated uncertainty. The results indicate that as the number of stations in the

combinations increases, the uncertainty decreases, because larger combinations consider more data and reduce the impact of noisy or unreliable data. Also, in combinations with fewer stations, the standard deviation is higher (approximately 0.0031). However, as the number of combinations increases, it decreases to about 0.0019.

Finally, figure 8 shows the analysis of high- rate GPS data on Anchorage 2018 earthquake.

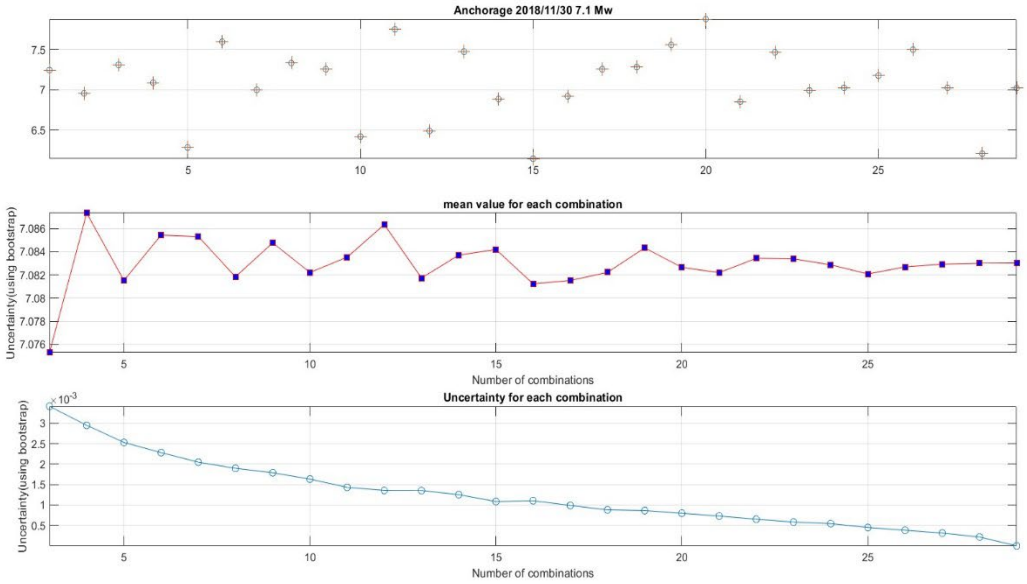

Figure 8- Magnitude estimation results for the Anchorage earthquake. The top panel shows the variation in magnitude values (y-axis) for different numbers of randomly selected stations (x-axis). The middle panel presents the distribution of magnitude estimates (y-axis) across multiple Bootstrap resampling combinations for each station count (x-axis). The bottom panel shows the standard deviation of the magnitude estimates (uncertainty, y-axis)) computed from the Bootstrap samples (x-axis).

In the first chart, the earthquake magnitude (M) for various GPS stations is shown. Each point in this chart represents the calculated magnitude for a specific combination of stations. The magnitude values vary in the range of 6.5 to 7.5. These variations are due to the different data recorded at each station and their geographical locations relative to the epicenter. These differences highlight the importance of combining data from multiple stations to achieve more stable results.

The second chart calculates and displays the average earthquake magnitude for various station combinations. As the number of stations in the combinations increases, the average earthquake magnitude approaches a more stable value (approximately 7.08). This convergence indicates a reduction in the impact of noisy or outlier data in larger combinations and points to greater stability in the results.

In the third chart, the standard deviation or uncertainty related to the earthquake magnitude for different station combinations is calculated and displayed using the Bootstrap method. It is observed that in combinations with fewer stations, the uncertainty is higher (approximately 0.004) and as the number of stations increases, the uncertainty significantly decreases and approaches about 0.0015. This reduction is due to the lesser impact of noisy data in the averaging of larger combinations.

In this study, all available GPS station data were used in the Bootstrap resampling process without applying any outlier exclusion or truncation. However, it is well known that extreme values—

due to noise, hardware malfunction, or local site effects—can distort averaging results. Seismological agencies such as NEIC commonly apply a truncation strategy, discarding 5–10% of the lowest and highest magnitude estimates to reduce this bias. Although this method was not implemented here, we acknowledge its potential benefits. Incorporating such a filtering approach in future analyses may improve the robustness and reliability of the final magnitude estimations.

The rate of uncertainty reduction varies between events. In particular, the Anchorage earthquake shows a more rapid decrease in uncertainty as the number of stations increases. This difference is not solely related to the earthquake magnitude, but rather to the spatial distribution of GPS stations. In the Anchorage case, stations were more evenly distributed around the epicenter, resulting in a smaller azimuthal gap. This circular coverage enhances the representativeness of sampled displacements and contributes to faster convergence in magnitude estimation. Conversely, the Tohoku and Chignik events exhibit less uniform azimuthal station distribution, which likely slowed the convergence of uncertainty.

Conclusion and Discussion

Analysis of high-sampling-rate GPS data for three major earthquakes—Tohoku (Mw 9.1), Chignik (Mw 8.2), and Anchorage (Mw 7.1) showed that the behavior of earthquakes and the quality of results are influenced by factors such as earthquake magnitude, focal mechanism, geographical location of stations, and data combination. Although factors such as earthquake magnitude, focal mechanism, and station distribution are known to influence the quality of magnitude estimation, this study specifically focused on analyzing the impact of data combination. Future work is recommended to comprehensively investigate the effects of the remaining factors.

The Tohoku earthquake, as a very large megathrust earthquake, showed more variability in the calculated magnitudes (8.5 to 9.5). In contrast, the Chignik and Anchorage earthquakes, being smaller, had a narrower range of variability. These differences are mainly related to the amount of energy released and the intensity of crustal displacement in these earthquakes.

Table 1 shows a comparison between the estimated values and the standard deviation values for all three earthquakes. It was observed in all three earthquakes that the average magnitude approaches a stable value with an increasing number of combined stations. For the Tohoku earthquake, this value was around Mw 9.25, for Chignik it was Mw 8.27, and for Anchorage it was Mw 7.08.

This behavior indicates a reduction in the impact of noisy data and achieving more stable results with an increasing number of stations in the combination. The faster convergence observed in the Anchorage earthquake is primarily attributed to the more uniform azimuthal distribution of GPS stations, which reduced the maximum azimuthal gap and led to more stable magnitude calculations, rather than solely due to the smaller earthquake magnitude.

In terms of uncertainty, the Tohoku and Chignik earthquakes, due to their larger magnitudes, had higher uncertainty in combinations with fewer stations (approximately 0.003). However, with an increasing number of stations, this value decreased to about 0.001. In contrast, the Anchorage earthquake, which was smaller and had more limited GPS data, showed a faster decrease in uncertainty. It is important to note that while the earthquake magnitude plays a role, the spatial distribution and density of GPS stations also have a significant impact on uncertainty reduction.

Specifically, a more homogeneous station distribution and better azimuthal coverage reduce uncertainty more effectively, regardless of the earthquake's magnitude. The slower uncertainty reduction observed for the Tohoku and Chignik events may also be attributed to less optimal

station coverage compared to the Anchorage event. An analysis of station distribution (Figures 5 to 7) indicates that denser and better-distributed stations improve magnitude estimation accuracy and stability. This finding emphasizes the importance of improving azimuthal coverage in tectonically active regions to achieve more reliable results.

In this study, all available GPS stations within the defined radius of each earthquake were included in the Bootstrap resampling process. We did not apply any explicit quality-control criteria to exclude noisy or faulty station data, nor did we define a fixed cutoff for the number of selected stations. While this comprehensive approach maximizes data utilization, it also introduces the possibility that outlier stations due to local noise, hardware malfunctions, or signal distortion—may bias the magnitude estimates. Currently, no stations were excluded from averaging based on signal quality or derived values. In future work, incorporating automated filtering strategies or a truncation approach such as excluding the top and bottom 5–10% of station-based estimates may help reduce the influence of extreme values and enhance the robustness and reliability of the results.

Table ¹ - Comparison between the estimated values and the standard deviation values for all three earthquakes"

Earthquake	Data Spread	Mean Magnitude Stability	Minimum Uncertainty (σ)	Maximum Uncertainty (σ)	Type	Magnitude (Mw)	Key Feature
Tohoku 2011	High (8.25 to 10.5)	~9.25	~0.0011	~0.0039	Megathrust	9.1	High energy release, large spread
Chignik 2021	Moderate (7.5 to 9)	~8.27	~0.0019	~0.0031	Megathrust	8.2	Moderate energy release, stable combinations
Anchorage 2018	Low (6.5 to 7.5)	~7.08	~0.0015	~0.004	Reverse fault	7.1	Smaller energy release, faster stability

In summary, these analyses show that high-rate GPS data, along with statistical methods such as Bootstrap, are powerful tools for estimating earthquake magnitude and analyzing uncertainty. Combining data from multiple stations not only increases the accuracy of the calculations but also reduces the impact of noisy or unreliable data. These results highlight the importance of using GPS data and advanced statistical analysis methods for more accurate earthquake assessment and crisis management.

References

Bakhtiari Asl, K., V. Plicka and K. Moghtased-Azar (2025). "Determining Apparent Source Time Function (ASTF) of Seismic Events through Empirical Green Function Analysis (A case study of Khoy 2023 earthquake) %J Iranian Journal of Geophysics." -.

Bilich, A., J. F. Cassidy and K. M. J. B. o. t. S. S. o. A. Larson (2008). "GPS seismology: Application to the 2002 M w 7.9 Denali fault earthquake." **98**(2): 593-606.

Bilich, A. L. (2006). Improving the precision and accuracy of geodetic GPS: Applications to multipath and seismology, University of Colorado at Boulder.

Boore, D. M., C. D. Stephens and W. B. J. B. o. t. S. S. o. A. Joyner (2002). "Comments on baseline correction of digital strong-motion data: Examples from the 1999 Hector Mine, California, earthquake." **92**(4): 1543-1560.

Chen, C., Z. Lai, R. C. Beardsley, J. Sasaki, J. Lin, H. Lin, R. Ji and Y. J. P. i. O. Sun (2014). "The March 11, 2011 Tōhoku M9. 0 earthquake-induced tsunami and coastal inundation along the Japanese coast: A model assessment." **123**: 84-104.

Colombelli, S., R. M. Allen and A. J. J. o. G. R. S. E. Zollo (2013). "Application of real-time GPS to earthquake early warning in subduction and strike-slip environments." **118**(7): 3448-3461.

Elósegui, P., J. Davis, D. Oberlander, R. Baena and G. J. G. R. L. Ekström (2006). "Accuracy of high-rate GPS for seismology." **33**(11).

Fang, R., C. Shi, W. Song, G. Wang and J. J. G. J. I. Liu (2014). "Determination of earthquake magnitude using GPS displacement waveforms from real-time precise point positioning." **196**(1): 461-472.

Gao, Z., Y. Li, X. Shan and C. J. R. s. Zhu (2021). "Earthquake magnitude estimation from high-rate GNSS data: A case study of the 2021 Mw 7.3 Maduo earthquake." **13**(21): 4478.

Hirahara, K., T. Nakano, Y. Hoso, S. Matsuo and K. J. G. 研. 集. Obana (1995). "An experiment for GPS strain seismometer." 67-76.

Konvisar, A., V. Mikhailov, V. Smirnov and E. J. I. Timoshkina, Physics of the Solid Earth (2024). "Postseismic processes in the region of the July 29, 2021 Chignik earthquake, Alaska: Part I. Modeling results." **60**(4): 543-553.

Lamarre, M., B. Townshend and H. C. J. B. o. t. S. S. o. A. Shah (1992). "Application of the bootstrap method to quantify uncertainty in seismic hazard estimates." **82**(1): 104-119.

Roberts, F. S. and B. Tesman (2024). Applied combinatorics, CRC Press.

West, M. E., A. Bender, M. Gardine, L. Gardine, K. Gately, P. Haeussler, W. Hassan, F. Meyer, C. Richards and N. J. S. R. L. Ruppert (2020). "The 30 November 2018 M w 7.1 anchorage earthquake." **91**(1): 66-84.

Salmanian, M., A. Rastbood and M. M. Hossainali (2025). "Evaluating interseismic deformation patterns in the North Tabriz Fault (Iran) using enhanced fitting of velocity field and analysis of surface deformation." Journal of Asian Earth Sciences **277**: 106376.